Sulfur passivation of semi-insulating GaAs: transition from Coulomb blockade to weak localization regime

© N.T. Bagraev *+, E.I. Chaikina•, E.Yu. Danilovskii*, D.S. Gets*, L.E. Klyachkin*,
  T.V. L'vova*, A.M. Malyarenko*

* Ioffe Institute,
194021 St. Petersburg, Russia
+ Peter the Great St.Petersburg Polytechnic University,
195251 St. Petersburg, Russia
• Division de Fısica Aplicada, Centro de Investigacion Científica y de Educacion Superior de Ensenada,
Carretera Ensenada-Tijuana No.3918, Ensenada,
Baja California, 22860 Mexico

E-mail: Bagraev@mail.ioffe.ru

The sulfur passivation of the semi-insulating GaAs bulk (SI GaAs) grown in an excess phase of arsenic is used to observe the transition from the Coulomb blockade to the weak localization regime at room temperature. The I−V characteristics of the SI GaAs device reveal nonlinear behavior that appears to be evidence of the Coulomb blockade process as well as the Coulomb oscillations. The sulfur passivation of the SI GaAs device surface results in enormous transformation of the I−V characteristics that demonstrate the strong increase of the resistance and Coulomb blockade regime is replaced by the electron tunneling processes. The results obtained are analyzed within frameworks of disordering SI GaAs surface that is caused by inhomogeneous distribution of the donor and acceptor anti-site defects which affects the conditions of quantum-mechanical tunneling. Weak localization processes caused by the preservation of the Fermi level pinning are demonstrated by measuring the negative magnetoresistance in weak magnetic fields at room temperature. Finally, the studies of the magnetoresistance at higher magnetic fields reveal the $h/2e$ Aharonov−Altshuler−Spivak oscillations with the complicated behavior due to possible statistical mismatch of the interference paths in the presence of different microdefects.

1. Introduction

Quantum dots (QDs), zero-dimensional systems, are obtained by fully confining the motion of charge carriers in quantum wires (QWrs), quantum wells (QWs), or in bulk crystals. Since the transport of charge carriers in a QD is confined in all directions, the corresponding energy spectrum is completely discrete, just as it is for an isolated atom [1]. For this reason, QDs are often called artificial atoms, although each QD consists of thousands or even hundreds of thousands of real atoms. Naturally, charged QDs are implied. Empty QDs cannot be considered as analogues of real atoms, but they are of special interest for studying the charge-carrier resonant tunneling through zero-dimensional systems [2]. In turn, like a real atom, a charged QD (an artificial atom) can contain one or several free charge carriers exhibiting both the confinement and electron-electron interaction effects during recharging [1]. Relative contributions of these effects are dependent on the size of a quantum dot and the characteristics of its boundary thereby forming the subsequence of shells revealed by studying the non-equidistant energy spectrum [3,4]. If the number of charge carriers in a QD is more than 100, the energy spectrum has to be equidistant and the distance between energy levels is determined by the electron-electron interaction controlled by varying the gate voltage, $E = e^2/C$, where C is the total capacitance of a QD [1,5–7].

Like QWs and QWrs, QDs can be obtained by combining as-grown samples by the molecular-beam epitaxial method and electrostatical gating using the nanolithography technique with subsequent selective etching and metal deposition of microcontacts [8,9]. For example, the formation of QDs inside the AlGaAs/GaAs heterostructures starts from the deposition of masks onto the surface of the wide-gap part, AlGaAs. The electrons from the shallow donor centers in AlGaAs transfer into the zero-dimensional GaAs dots prepared by etching. Therefore, the number of charge carriers localized in a QD is determined by the shallow donor concentration which is unfortunately suppressed by their self-compensation due to the replacement of the Ga neighboring atom by Al that results in the formation of the DX centers [10,11]. This self-compensation in as grown structures gives rise to difficulties in studies of the energy and charge quantization phenomena. However, this disadvantage can be eliminated in electrostatically prepared one-dimensional and zero-dimensional structures in which the motion of the charge carriers in QWs is confined by the voltage applied to the microcontacts (Fig. 1, a). The main advantage of electrostatic methods is the ability to increase and control the number of electrons or holes in a QD up to several hundreds, thus allowing the observation of the changes in the current-voltage (I−V) characteristics that appear to reveal the Coulomb blockade and Coulomb oscillations [12].

By varying the source-drain voltage (V_{ds}) and the gate voltage (V_g), we can create not only the QWr connecting two $2D$ lakes using the split-gate technique but also form a QD inside this quantum wire (Fig. 1, a) [9]. These electrostatic QDs result from the voltage applied to finger
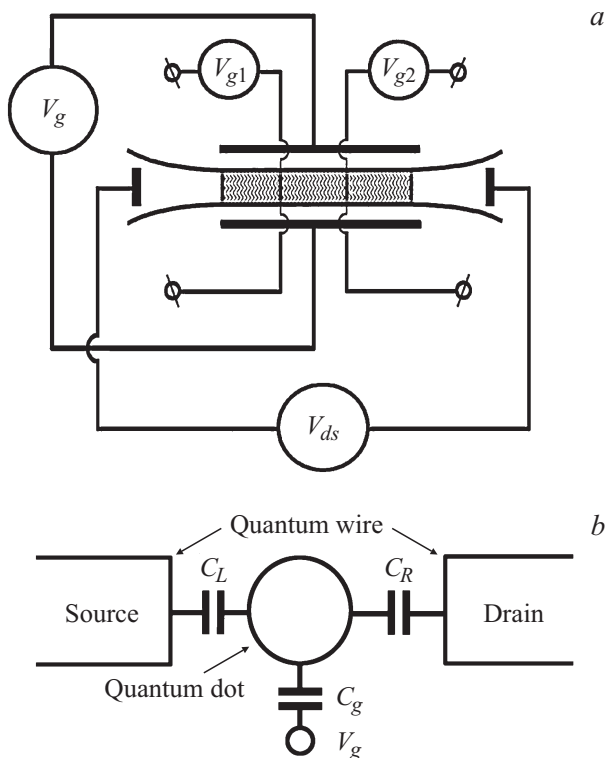
Figure 1. *a* — a schematic representation of the structure designed for studying the Coulomb blockade, Coulomb oscillations, and Coulomb staircase of the conductance of a quantum dot during the transport of single charge carriers. The split-gate voltage, V_g, is used to create the modulated QWr inside QW. The voltages V_{g1} and V_{g2} are applied to the finger gates to define a quantum dot. *b* — a scheme for a weakly coupled quantum dot inside a quantum wire.

gates, whereas the central gate voltage controls the number of 1D sub-bands below the Fermi level (Fig. 1, *a*). Thus, the scheme that is able to control the I−V characteristics of a QD inside electrostatic QWr appears to be a basis of the variety of single electron transistors [13–15]. Such a system where single electron tunneling (SET) can be observed consists of the drain, source and the island that is isolated from controlling gates (Figs 1, *a, b*).

The tunneling processes through the isolated island (or series of isolated islands) could be suppressed if low voltage is applied to the drain-source contacts as a result of the Coulomb blockade which arises from the Coulomb interaction of the tunneling electron with the electrons captured at a quantum dot (Fig. 1, *b*). Therefore the island can be recharged by varying the integer number of electrons when the gate voltage drops across the island as well as the drain-source voltage appears to be changed. These procedures result in charge imbalance between the drain-source contacts and the isolated island, which shows up in saw-tooth like oscillation depending on the gate voltage value [1]. The transport through the island is forbidden everywhere except the points of saw-tooth dependent changes from $+e/2$ to $-e/2$, in which the Coulomb blockade is lifted, and the

conductance exhibits a peak. Thus, the conductance of such a device oscillates depending on the gate voltage value, with the period equal to the value of $\Delta V_g = e/C_g$, where C_g is the gate capacitance (see Fig. 1, *b*).

Besides, the I−V characteristics reveal the threshold behavior for the electron tunneling processes, $eU_{th} = e^2/2C$, where C is total capacitance of the device which represents the sum of the gate capacitance (C_g) and the capacitance of the island (C_i) that contains also the capacitances of the left and right leads (see Fig. 1, *b*), $C = C_i + C_g = (C_L + C_R) + C_g$ [16, p. 306]. The Coulomb blockade is overcome when the quasi-Fermi levels are formed by increasing the value of the V_{ds} voltage. Furthermore, the changes of the quasi-Fermi level appear to exhibit the energy position of the zero-dimensional sub-bands [1]. The current begins to flow as soon as the Fermi level of the source rises above the first zero-dimensional sub-band [12]. When the Fermi level rises further, the higher zero-dimensional sub-bands begin to contribute to the current [1].

It's necessary to note that there are no fundamental reasons forbidding the observation of the Coulomb blockade at high temperature. Moreover, recently the Coulomb blockade has been observed around room temperature [17]. It requires a significant energy difference between neighboring Coulomb energy levels in comparison with thermal energy, $\Delta E = e^2/2C > kT$, or, in another words, a realization of the small capacitance system due to decrease of the quantum dots size as well as the QDs serial sequences formation. Besides, tunneling resistance (R_T) has to be much greater than quantum resistance (R_K), h/e^2, $R_T \gg R_K$, thereby confining the electron wave function to an isolated island [16,18]. From this point, the surface of semi-insulating GaAs prepared in an excess phase of arsenic is a very interesting model material because it can be represented as a strong disordered system of the charged and uncharged quantum dots formed from the anti-site related defects. If such surface disordering could be controlled somehow, the transition from the Coulomb blockade regime to the weak localization regime would be possible to observe at high temperatures, because the conditions of quantum-mechanical tunneling depend on degree of disorder. Here the goal of this work is to study these phenomena on the surface of the semi-insulating GaAs bulk (SI GaAs) using the sulfur passivation technique.

2. Methods

The experimental samples were the SI GaAs bulk crystals obtained in an excess of arsenic. The measurement of the I−V characteristics were performed in the Hall bar geometry, 4.7×0.2 mm, at room temperature. The gold contacts, 0.2×0.2 mm, were prepared making a mask with subsequent photolithography procedure to measure the longitudinal voltage drop, U_{xx}, during the DC current sweep at different magnitudes of the gate voltage. The DC current
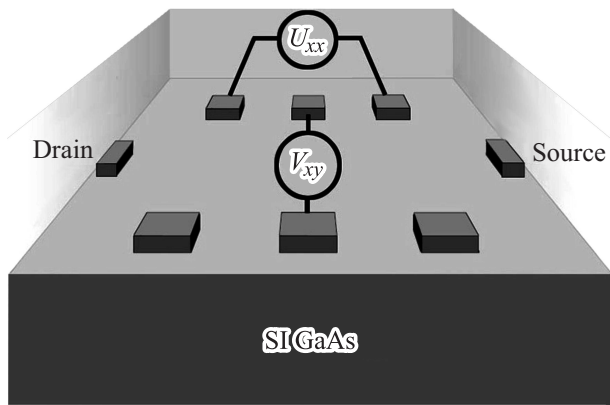
Figure 2. A device scheme designed to study the electrical properties of the surface of SI GaAs bulk. The I−V ($U_{xx} = f(I_{ds})$) characteristics were measured under the gate voltage applied to the U_{xy} contacts.

was applied to the source-drain contacts, I_{ds}, within frameworks of the Hall bar geometry (Fig. 2). The gate voltage, V_g, was applied to the U_{xy} contacts transversely to the I_{ds} current. The U_{xx} voltage drop was measured by the voltmeter (Keithley 6517A) with extremely high impedance.

After measuring series of the I−V characteristics, the samples were passivated by sulfur. Prior to sulfur passivation, the samples were rinsed in acetone and 2-propanol and subsequently treated with 1M aqueous sodium sulfide solution for 4 min. Then, the same sequence of the I−V characteristics was repeated as well as the magnetoresistance was measured by the Hall method at room temperature.

3. Experimental results and discussion

3.1. Coulomb blockade

Series of the I−V characteristics obtained at room temperature reveal nonlinear behavior that appears to be evidence of the Coulomb blockade process (Fig. 3). It is mentioned above that the total capacitance of the Coulomb blockade system, C, is the sum of the gate capacitance, C_g, and the capacitance of the island, C_i, (see Fig. 1, b), $C = C_i + C_g$ [16, p. 306]. Thus, both capacitances, C_i and C_g, are necessary to be estimated. Linear approximation of high current gives the voltage threshold value of $U_{th} = 0.68 \pm 0.02$ V which results from the Coulomb blockade condition, $eU_{th} = e^2/2C$ (Fig. 3). Therefore, the total capacitance, C, can be estimated as $(1.18 \pm 0.03) \cdot 10^{-19}$ F. Moreover, as noticed above the gate capacitance appears to be defined from the period of the Coulomb oscillations, $\Delta V_g = e/C_g$, revealed by measuring the U_{xx} voltage as a function of the gate voltage, V_g (Fig. 4). Fig. 4 shows the oscillations with a period of 1.5 ± 0.25 V that corresponds to the value of the gate capacitance equal to $(1.07 \pm 0.18) \cdot 10^{-19}$ F.

Thus, the island capacitance, $C_i = C - C_g$, appears to be equal to $(1.1 \pm 0.2) \cdot 10^{-20}$ F. If the island is assumed to be spherical form, its radius is estimated as $r = C_i/8\varepsilon_0\varepsilon \approx 0.13 \pm 0.02$ Å, where $\varepsilon = 12$ for GaAs, $\varepsilon_0 = 8.85 \cdot 10^{-12}$ F/m. But this value is too small even if the Coulomb blockade could be caused by only single point defect. This result a reason for doubt to use the spherical model at nanoscale. Therefore, such a capacitance value seems to result from the serial concatenation of capacitors:

$$1/C = 1/C_1 + \ldots + 1/C_n \approx n/C_0, \qquad (1)$$

where C_0 is the capacitance of single element in a chain.

As it was mentioned above, to observe the Coulomb oscillations at room temperature it is necessary to achieve
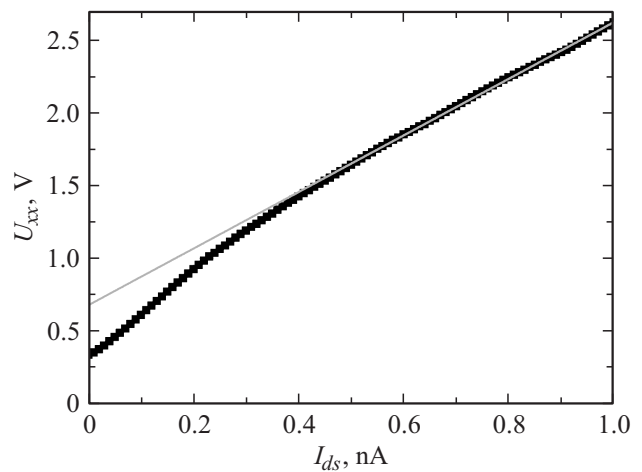

Figure 3. The I−V characteristic measured at the surface of the semi-insulating GaAs bulk structure. Solid line indicates the Coulomb blockade threshold, $U_{th} = e/2C$. $T = 300$ K.
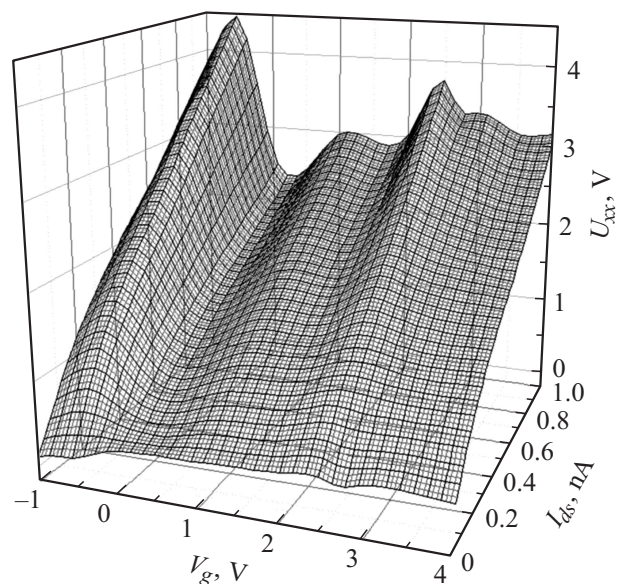

Figure 4. 3D plot of the Uxx voltage measured at the surface of the semi-insulating GaAs bulk structure at different values of the gate-voltage and the drain-source current. $T = 300$ K.
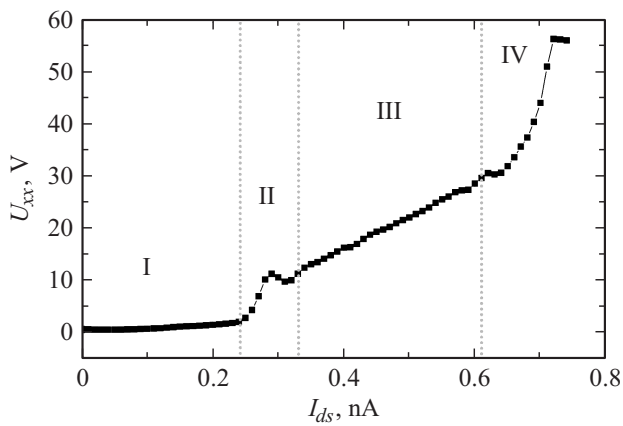
Figure 5. The I−V characteristic after passivation of the SI GaAs bulk crystal by sulfur. $T = 300$ K; $V_g = 0$.

low capacitance value of an island. However, the total capacitance of serial concatenation of islands overall, $C = C_0/n$, can be rather small. Such capacitor systems seem to represent microdefects, dislocations, clusters or extended defects. The anti-site related centers, As_{Ga}, appear to be very good candidates to play an important role in the Coulomb blockade phenomena because of their high concentration on the surface of the SI GaAs bulk crystals grown in an excess of arsenic [19–24]. The serial arrangement of the single capacitors was suggested to be caused by the deformation potential introduced by the contacts which are able to create preferable direction of the anti-site defects packing on the GaAs surface.

The question arises on the restriction of the number of capacitors in a chain to justify the serial concatenation
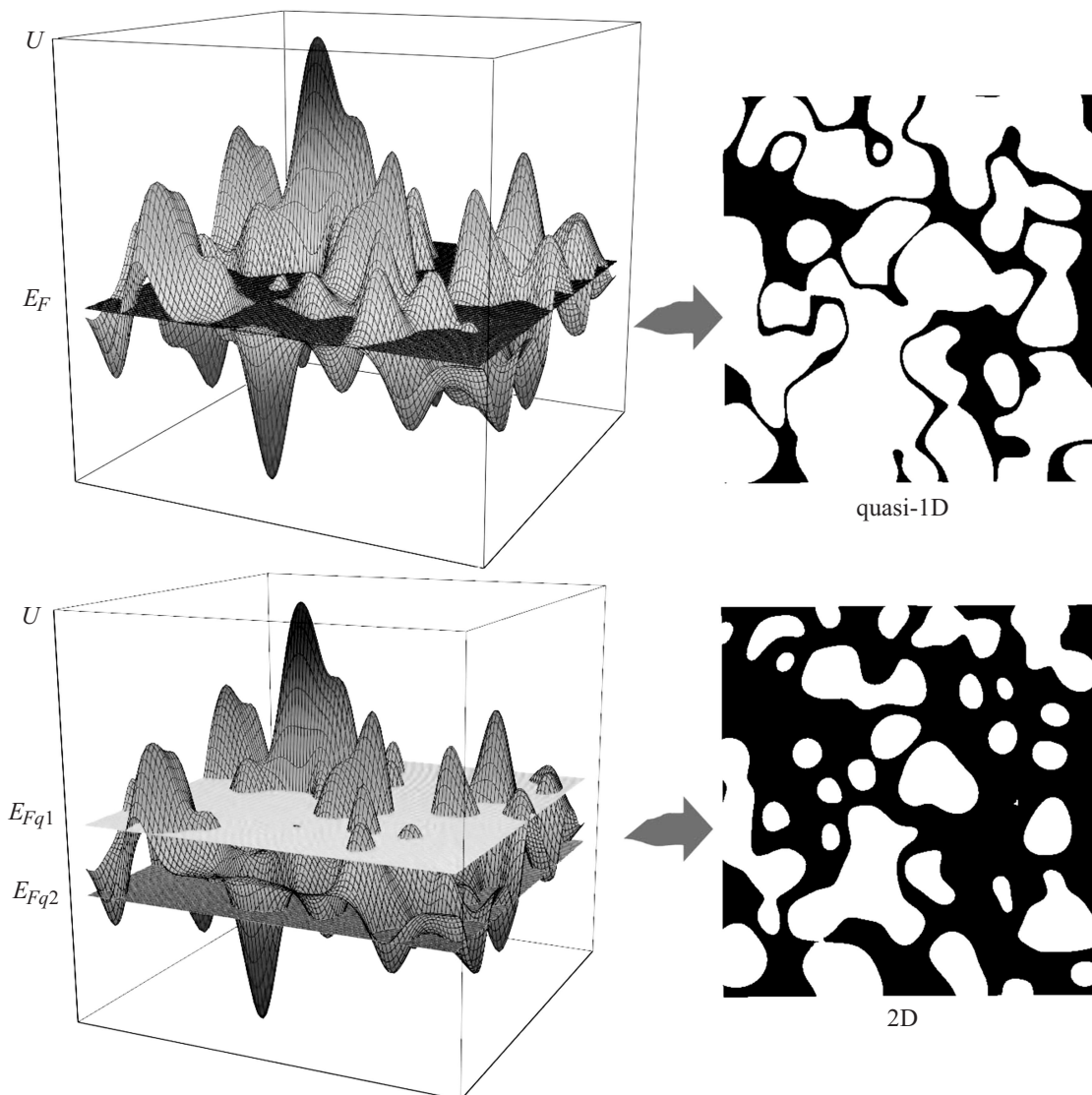

Figure 6. Schematic diagram of the potential profile at the Fermi level position for the SI GaAs surface after passivation by sulfur. Chaotic sequence of the surface defects before and after passivation by sulfur results in the complicated system of the potential barriers that seems to be a basis of the resistance increase. Owing to the position of the quasi-Fermi levels the transport processes have to crossover from the quasi-1D to the 2D regime, whereas the conductance is controlled by scattering on random potential between the E_{Fq1} and E_{Fq2} energies.
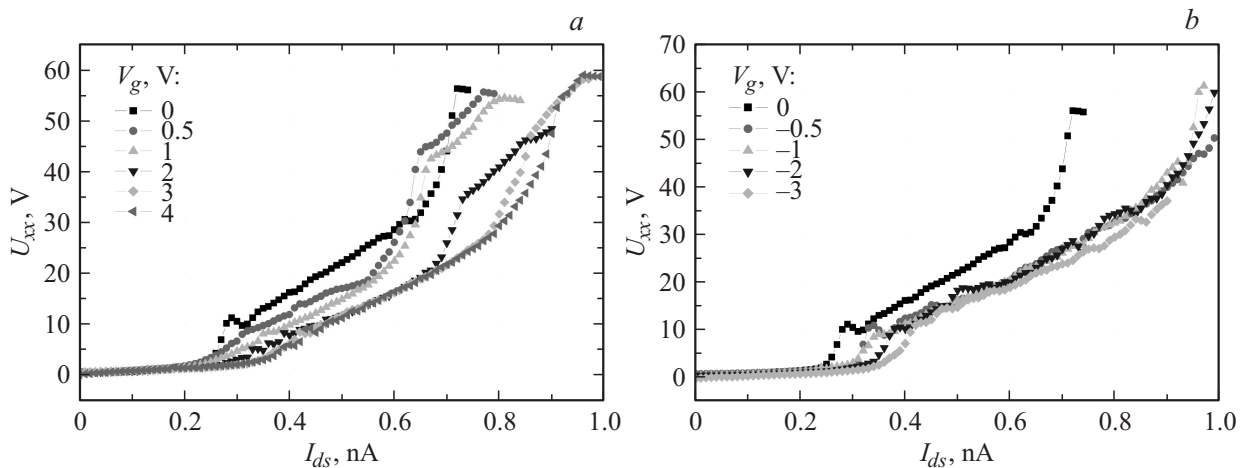
Figure 7. I−V characteristics of the SI GaAs sample passivated by sulfur under applied positive (*a*) and negative (*b*) gate-voltage $T = 300$ K.

model. This value seems to be up to 10^5, if the sheet density of the anti-site defects near the SI GaAs surface to be taken into account. Nevertheless, the degree of disorder in the defect's arrangement has to be a more effective factor to enhance the Coulomb blockade in such a system. Therefore, the suppression of the charge activity of the anti-site defects which appears to give rise to the changes in the relation between their charged and uncharged states can cause the transition from the Coulomb blockade to the resonant tunneling regime. In order to control this relation that affects the degree of disorder, the passivation of the SI GaAs by sulfur was used. The measurements of the I−V characteristics as well as the magnetoresistance were carried out to identify the parameters of the tunneling and weak localization processes.

3.2. Tunneling transitions

Fig. 5 shows that the sulfur passivation results in enormous transformation of the I−V characteristics. Firstly, the resistance of the SI GaAs device studied has increased significantly. Secondly, the I−V characteristic demonstrates four different ranges. Two of them are described by the linear ohmic dependence versus applied current (see the ranges I and III). It should be noted that the resistance in the second ohmic part is much higher than in the first one. Another two ranges are related to the transition process that is defined by the presence of the Negative Differential Resistance (NDR) (see the ranges I and IV). The following model can qualitatively describe this behavior. Within the suggested model anti-site defects are transformed into electrically neutral centers as a result of the sulfur passivation. These electrically neutral centers represent some potential barriers for charge carriers. Thus, the transport along the device surface is defined by the tunneling processes through these potential barriers. Therefore, the surface resistance after sulfur passivation increases dramatically in comparison with that of initial samples before this procedure

(see range I in Fig. 5). The I_{ds} change from 250 pA to 280 pA results in a sharp resistance increase in this range due to scattering events of carriers on the potential barriers (range II in Fig. 5). Then, the tunneling probability for the charge carriers is enhanced which is revealed by the S-shaped I−V characteristics in the I_{ds} range from 290 pA to 310 pA as within frameworks of the Esaki model [25]. The range III in Fig. 5 shows the characteristic ohmic behavior of $U_{xx}(I_{ds})$, because the value of the resistance is dependent on the scattering processes, whereas its fluctuations are manifested by the tunneling processes. Therefore, the difference in the chemical potentials of the I_{ds} contacts gives rise to the conductance that is affected by scattering on random potential between energies E_{Fq1} and E_{Fq2}, and owing to the creation of the quasi-Fermi levels the transport processes appear to crossover from the quasi-1D to the 2D regime (Fig. 6). However, the resistance of such a system seems to be increased as a result of the localization of carriers in the traps introduced by random potential of the SI GaAs surface passivated by sulfur. The high I_{ds} range in the I−V characteristics is defined by the break down of the device into the insulator regime with the values of resistance up to 60 GΩ (see range IV in Fig. 5). Finally, such a break down behavior for the I−V characteristics has to be evidence of further increase of the difference between energies E_{Fq1} and E_{Fq2} that can be a reason for a giant gain in scattering power of random potential.

The results of the series of I−V characteristics measured under different applied gate voltages using the Hall contacts are presented in Figs 7, *a, b*. The NDR area is found only at $V_g = 0$ (see Fig. 5). For both positive and negative gate voltage applied to the device, the break down point to an insulator regime is shifted to higher I_{ds} values accompanied by the disappearance of the main NDR peak (see Figs 7, *a, b*). This result is possiblly the evidence of identical parameters of all tunnel barriers created by the sulfur passivation and seems to be due to the stabilization of the quasi-Fermi level position on the SI GaAs surface when
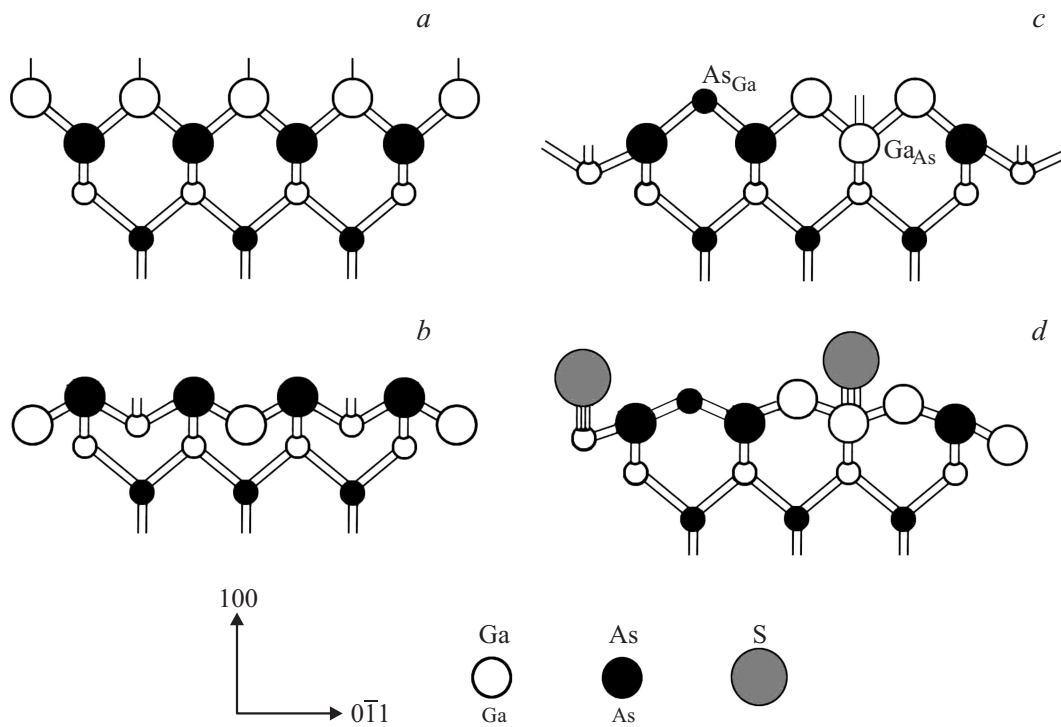
Figure 8. Model of the (100) face of the GaAs sample (a) reconstructed because of the negative-U properties for the Ga dangling bonds (b) and the Ga$_{As}$ double acceptor anti-site centers in the presence of the As$_{Ga}$ surface donor anti-site defects (c), which promote the sulfur adsorption processes (d).

the critical value of I_{ds} is reached for the next tunneling barrier. Besides, the redistribution of the potentials inside the serial concatenation of the tunneling barriers when the I_{ds} value is scanning can result from the higher charge carrier velocity that gives rise to the increase of resistance as a result of intensive scattering processes.

As noticed above, these results testifying to the transition from the Coulomb blockade regime to the quantum-mechanical tunneling on a SI GaAs surface can be considered within frameworks of the model of the surface defects passivated by sulfur. The donor (As$_{Ga}$) and acceptor (Ga$_{As}$) anti-site related centers as well as the Ga dangling bonds are known to be responsible for the self-compensation processes that are a basis of the growth of different varieties of SI GaAs [20,21,26,27]. The self-compensation results in the Fermi level pinning at a SI GaAs surface and make the passivation by the elements with two excess electrons possible, for example, chalcogens, because these centers are respectively double donors (As$_{Ga}$$(+/++) - E_v + 0.52$ eV; As$_{Ga}$$(0/+) - E_c - 0.75$ eV) [23], double acceptor (Ga$_{As}$$(0/-) - E_v + 0.077$ eV; Ga$_{As}$$(-/--) - E_v + 0.2$ eV [21,28]). However the studies of the negative electron affinity formation at the GaAs surface under the passivation by cesium and oxygen have revealed the opposite order for the acceptor levels in the gap (Ga$_{As}$$(-/--) - E_v + 0.077$ eV; Ga$_{As}$$(0/-) - E_v + 0.2$ eV) [21]. Therefore, this center as well as the amphoteric Ga dangling bond center

$((0/+) - E_c - 0.2$ eV; $(-/0) - E_v + 0.25$ eV) appear to be very good candidates for the passivation of the SI GaAs surface because of their negative-U properties [29–31] (see Figs 8, a–d and 9, a). Since the Fermi level pinning is enhanced in the presence of the negative-U centers, their effect on the compensation of the anti-site donor centers seems to give rise to the Coulomb blockade in the impurity bands (Figs 9, b, c). Moreover, the inhomogeneous distribution of the donor and acceptor anti-site centers has to lead to the parallel and series concatenation of the charge islands confined by the barriers which appear to be revealed by studying the I−V characteristics (see Figs 3 and 4). Fig. 9, c demonstrates these disorder effects with the charge islands caused by the self-compensated surface area with the neutral donor anti-site centers appearing in between. In turn, the role of the passivation of the negative-U centers that suppresses the Coulomb blockade effects is shown in Fig. 9, d as the energy barrier's smoothing at the preservation of the Fermi level pinning. Under these conditions the Coulomb blockade transport regime seems to be replaced by the electron tunneling from the neutral anti-site donors by hopping processes through compensated surface area that contains the one-electron As$_{Ga}^+$ centers (see Fig. 9, d). Within frameworks of the model presented the distance between the quasi-Fermi energies E_{Fq1} and E_{Fq2} that appear to be affected by scattering on random potential results from the energy barrier between the As$_{Ga}^0$ and As$_{Ga}^+$ states (see Fig. 6). Thus, the surface areas passivated by
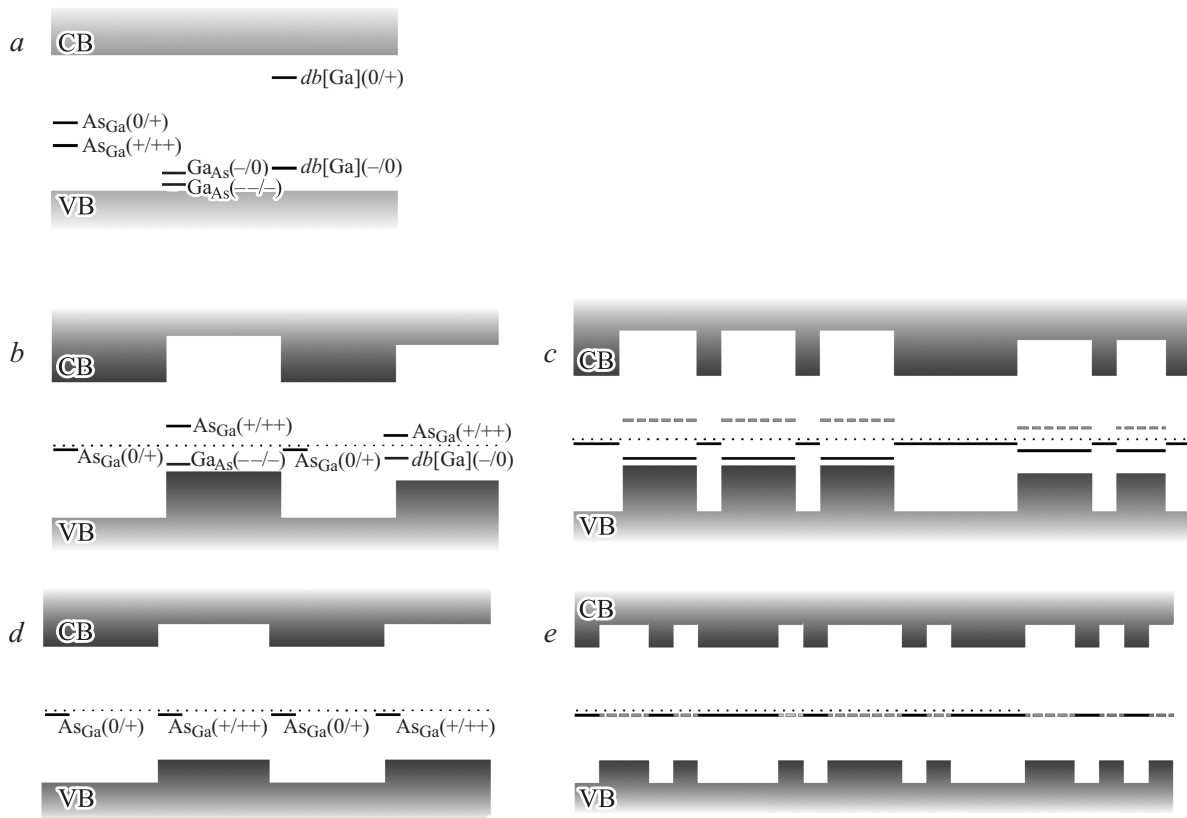
Figure 9. One-electron band scheme which demonstrates the energy level positions for the double donor As_{Ga} and acceptor Ga_{As} anti-site centers as well as the amphoteric Ga dangling bond center (*a*), the Fermi level pinning caused by the inhomogeneous distribution of the acceptor centers (*b*), the Coulomb blockade transport regime that results from the formation of the charge islands confined by the barriers containing the neutral donor anti-site centers (*c*), the preservation of the Fermi level pinning after the passivation of the SI GaAs surface by sulfur (*d,e*).

sulfur have to be the object in which the processes of the weak localization can be observed because of the Fermi level pinning. The studies of the weak localization processes seem to give evidence for their sizes which appear to be a reason for of the I−V characteristics shown in Figs 3−5 and 7, *a, b*.

In order to verify the processes of weak localization in the GaAs surface areas passivated by sulfur, the measurements of magnetoresistance were performed within the Hall geometry at room temperature at two values of the drain-source currents (100 pA and 1 nA). The results obtained are shown in Fig. 10. Each point was measured 50 times to increase the accuracy of the experiment. The error bars were calculated taking into account 0.95 confidence interval. Both curves demonstrate the negative magnetoresistance behavior in weak magnetic fields ($B < 300$ G) that appears to be the manifestation of the weak localization regime realized in disordered systems, where the charge motion is diffusive ($l_\varphi \gg l_m$, l_φ — phase coherence length, l_m — the mean free path) rather than ballistic. In this case the weak localization correction ($\Delta\sigma$) comes from the quantum interference between self-crossing paths in which an electron can propagate in the clock-wise and counter-

clockwise direction around a loop that contains series of scatters (see insert in Fig. 11) [32,33]. The change observed in the value of conductance appeared to be less than 1% of $e2/h$ although the relative variations of the resistance are of the order 30%, with the absolute values of the resistance shown in insert of Fig. 10. The behavior of the magnetoresistance measured at $I_{ds} = 100$ pA in weak magnetic fields seems to be described satisfactory by well-known formula for a weak localization in narrow channels [34,35]:

$$\Delta R(B)/R = -R/L \cdot 2e^2/h[(1/l_\varphi^2 + W^2/12l_B^4)^{-1/2} - l_\varphi], \quad (2)$$

where W — channel width, $l_B = (h/4\pi eB)^{1/2}$, $W < l_B$. The result of two-parameter fitting (W and l_φ) is shown in Fig. 11, *a*, $W = 10.6 \cdot 10^{-9}$ m, $l_\varphi = 0.92 \cdot 10^{-6}$ m, $L = 2$ mm, $R = 200$ MΩ, $l_B = 10^{-7}$ m at $B = 300$ G. However, two questions arise. Why weak localization is observed at room temperature and what is the cornerstone of so large value of the phase-relaxation length (l_φ) for the SI GaAs surface passivated by sulfur.

The magnetoresistance curves with positive convexity are specific to 1D transport [34]. Probably therefore it is rather difficult to analyse the data presented in Fig. 10
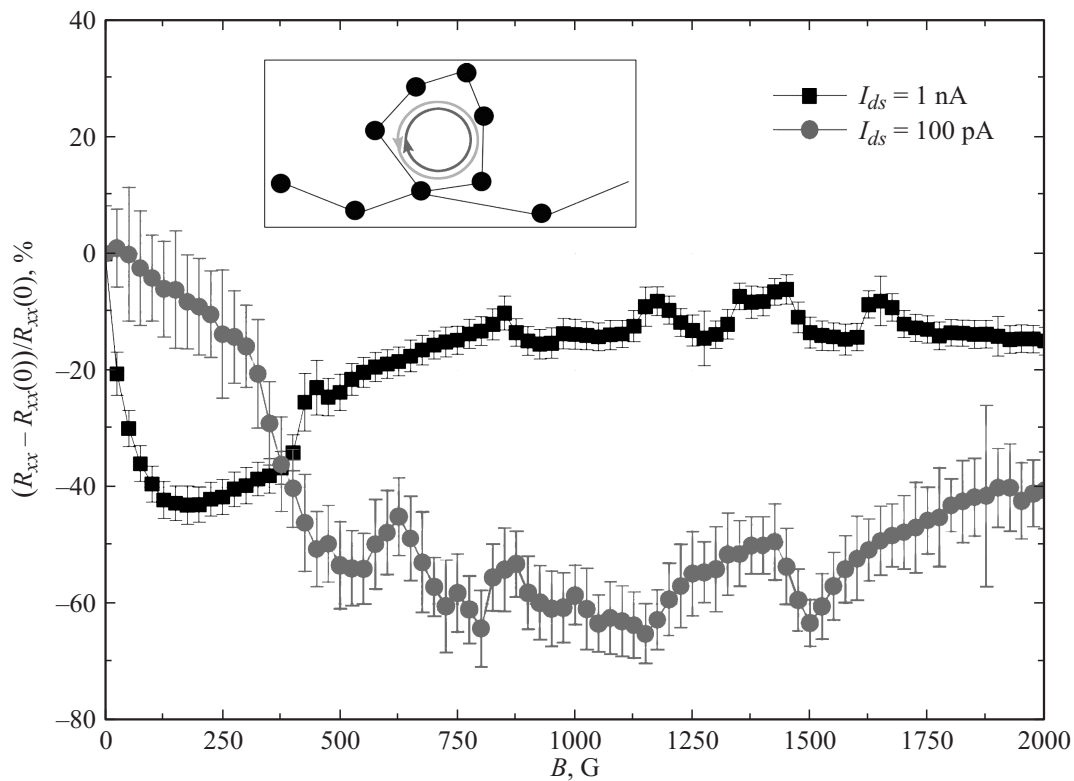
Figure 10. Relative magnetoresistance changes of the SI GaAs sample passivated by sulfur which were measured at two values of the drain-source current at $T = 300$ K. Insert: The loop containing series of scatters that result in the quantum interference between self-crossing paths in which an electron can propagate in the clock-wise and counter-clockwise direction.

within frameworks of the weak localization models for the 2D systems [36,37]. If the values of the sheet density, $n_{2D} = 7.25 \cdot 10^9$ m^{-2}, and mobility, $\mu = 0.5$ m^2/Vs, see also [26] are taken into account, then the transport time, $\tau_m \sim 2 \cdot 10^{-13}$ s, is rather small than the phase relaxation time, $\tau_\varphi = l_\varphi^2/D = 2 \cdot l_\varphi^2/v_F^2 \tau_m \sim 4 \cdot 10^{-6}$ s, that gives rise to that condition of a weak-localization regime.

At higher magnetic fields (> 500 G), the magnetoresistance measured at $I_{ds} = 100$ pA reveals the oscillations that appear to be a result of the $h/2e$ Aharonov–Altshuler–Spivak (AAS) effect, with the complicated behavior because of possible statistical mismatch of the interference paths in the presence of different microdefects [33,38]. The average period of the high magnetic field oscillations is estimated by the following approach. Firstly, the accurate maxima positions are obtained by the decomposition of the oscillations into several Lorentz-shape peaks. The results of this decomposition are presented in the Table. The estimated average period is equal to $\Delta B = 200 \pm 38$ G. Since the error is significant, the low-frequency signal part was filtered by the Savitzky-Golay digital filter with the window corresponding to the value of $\Delta B = 200$ G. The results of the low-frequency filtering give rise to the residual oscillations with the period $\Delta B = 181 \pm 5$ G that is in a good agreement with data obtained in the first step (see Table). From this behavior we can estimate the average

size of the defect area responsible for the magnetoresistance oscillations. Taking into account the phase relation for the closed circuit we can write: $2\Phi/\Phi_0 = 1$, $\Phi = \Delta B \cdot S$, $S = \Phi_0/(2\Delta B) \approx (5.7 + -0.2) \cdot 10^{-14}$ m^2, if $\Delta B \approx 181$ G. Then, the approximate AB-loop size ($r = \sqrt{S/\pi}$) is about 135 ± 4 nm. This size could be attributed to the SI GaAs surface compensated as a result of the sulfur passivation [30,31,39]. It should be noted that the average value of the weak localization resistance drop is close to the period of the magnetoresistance oscillations (see Fig. 11, a).

The magnetoresistance dependence measured at $I_{ds} = 1$ nA show similar trend, but the behavior in weak magnetic fields becomes more abrupt and the sign of

The results of the magnetoresistance decomposition by the Lorentz-shape peaks

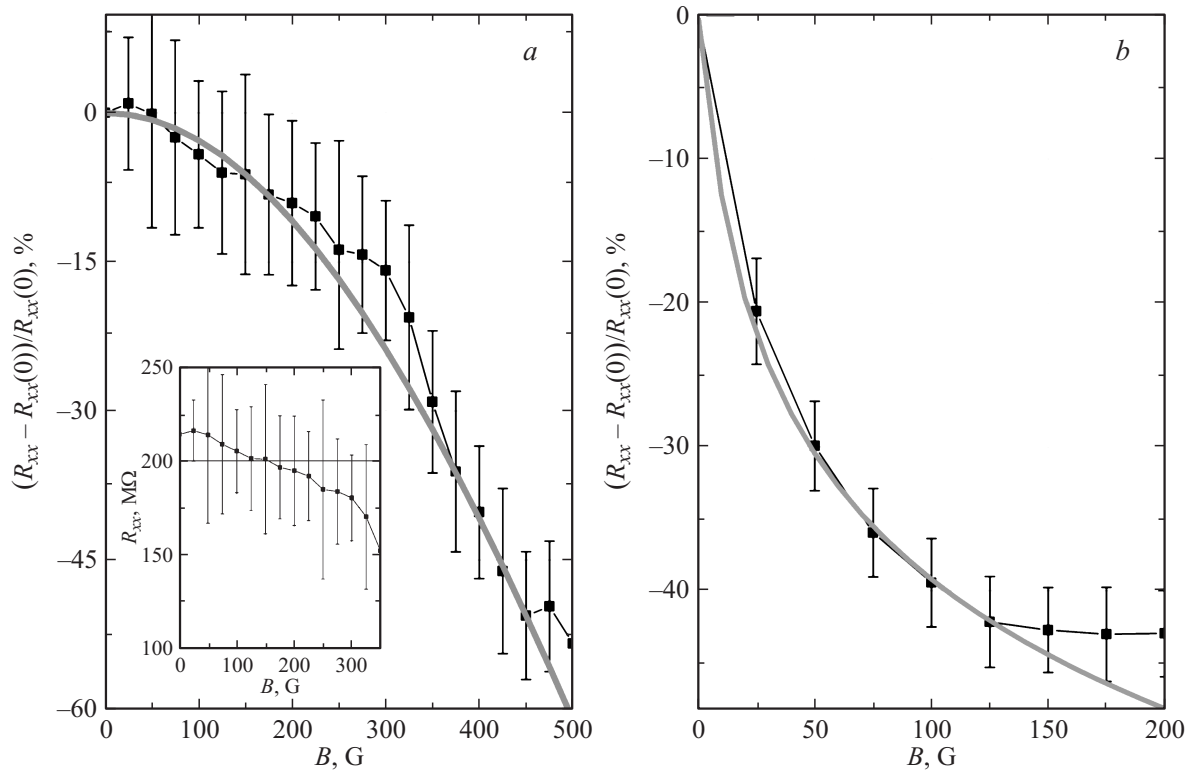| Peak #	Peak position, G	Standard Deviation, G	Distance between the neighbor peaks, G
1	490.6	8.4	274.0
2	764.7	5.5	177.1
3	941.7	7.9	175.6
4	1117.3	9.2	202.0
5	1319.3	27.6	184.6
6	1503.9	4.3	181.3
7	1685.2	60.7	

Figure 11. *a* — relative magnetoresistance of the SI GaAs sample passivated by sulfur that is measured at low value of $I_{ds} = 100$ pA ($T = 300$ K). The absolute resistance values are demonstrated in insert. The solid curve is theoretical fitting based on Eq. (2). *b* — relative magnetoresistance of the SI GaAs sample passivated by sulfur that was measured at high value of I_{ds} ($T = 300$ K). The solid curve is theoretical fitting based on Eq. (3). $I_{ds} = 1$ nA.

convexity changed (Fig. 11, *b*). According to Ref. [34], it could be a result of a transition from quasi-1D channel to 2D channel [40]. In the case of the 2D channel ($W \gg l_B$) the fitting procedure in the frameworks of the model described above [36,37] is difficult because there are three independent parameters, but in weak magnetic fields ($B < B_{th} = h/8\pi e D\tau_m$), for a weak spin-orbit interaction and a weak magnetic scattering we can use the formula:

$$\Delta R(B)/R = -R \cdot W/L \cdot e^2/\pi h[ln(B_\varphi/B)$$
$$-\psi(1/2 + B_\varphi/B)], \qquad (3)$$

where ψ-digamma function, $B_\varphi = h/8\pi e l_\varphi^2$ [36]. Fitting result is also presented in Fig. 11, *b*, with $l_\varphi = 1.46$ mkm, $W = 54$ mkm. Compared to the result obtained at $I_{ds} = 100$ pA, the value of W has increased that is in a good agreement with 1D-2D transition model.

Further increase of the magnetic field results in the linear positive magnetoresistace response measured at $I_{ds} = 1$ nA (Fig. 10). This linear magnetoresistace effect is a property of compositionally inhomogeneous semiconductors with strong electrical disorder [41]. These systems could be described within frameworks of the classical model of the 2D resistor network that mimic inhomogeneous conducting media [42]. At higher magnetic field, the magnetoresistance oscillations are observed as well as for $I_{ds} = 100$ pA. The

period value obtained from sinus fitting appeared to be of the same order ($\Delta B = 121 \pm 8$ G) as in those oscillations. To sum up, the increase of I_{ds} leads to the change from the quasi-1D transport to the 2D transport. This transition attributes the increase of the system resistance as it was seen in the I−V characteristics, where the first part (I, see Fig. 7) has lower resistance than the third part (III, see Fig. 7). As it was mentioned above, the weak localization effects were observed at room temperature. Previously, the weak localization characteristics have already been seen at room temperature in graphene grown on the SiC surface by CVD and in SI GaAs under LED illumination [43,44]. The SI GaAs surface passivated by sulfur seems also to be a good candidate for the observation of a weak localization at room temperature because of the preservation of the Fermi level pinning due to the presence of the deep level defects like donor and acceptor anti-site defects [45].

4. Summary

The sulfur passivation of the semi-insulating GaAs bulk, prepared in an excess phase of arsenic has been used to observe the transition from the Coulomb blockade to weak localization regime at room temperature. It became possible as the conditions of quantum-mechanical tunneling appeared to depend on the degree of disorder of the SI GaAs surface

that is caused by inhomogeneous distribution of the donor and acceptor anti-site defects.

The I−V characteristics of the SI GaAs device have revealed nonlinear behavior that appears to be evidence of the Coulomb blockade process as well as the Coulomb oscillations that are observed by measuring the dependence of the longitudinal voltage on the gate voltage applied to the Hall contacts under high stabilization of the drain-source current. The sulfur passivation results in enormous transformation of the I−V characteristics that demonstrate the strong increase of the resistance of the SI GaAs device which is due the localization of carriers in the traps introduced by random potential.

The results obtained have been analyzed within frameworks of the self-compensation of the donor and acceptor anti-site defects as well as the amphoteric Ga dangling bonds that are very good candidates for the passivation by the elements with two excess electrons, for example, chalcogens, because of their negative-U properties. Since the Fermi level pinning is enhanced in the presence of the negative-U centers, their effect on the compensation of the anti-site donor centers seems to give rise to the Coulomb blockade in the impurity bands. Moreover, the inhomogeneous distribution of the donor and acceptor anti-site centers has to lead to the parallel and series concatenation of the charge islands caused by the self-compensated surface area which are confined by the barriers that contain neutral anti-site donors. The I−V characteristics have shown that sulfur passivation of the negative-U centers suppresses the Coulomb blockade effects because of the energy barrier's smoothing at the preservation of the Fermi level pinning. Thus, the Coulomb blockade transport regime seems to be replaced by the electron tunneling from the neutral anti-site donors by hopping processes through compensated surface area that contains the one-electron As_{Ga}^{+} centers.

The preservation of the Fermi level pinning has revealed the SI GaAs surface areas passivated by sulfur as the object for the studies of the weak localization processes that have been demonstrated by measuring the negative magnetoresistance in weak magnetic fields at room temperature. These results appear to be the manifestation of the weak localization regime realized in disordered systems, where the charge motion is diffusive rather than ballistic. At higher magnetic fields, the magnetoresistance measurements have revealed the oscillations that appear to be a result of the $h/2e$ Aharonov−Altshuler−Spivak effect with the complicated behavior because of possible statistical mismatch of the interference paths in the presence of different microdefects. The AB-loop size estimated from the period of the AAS oscillations could be attributed to the SI GaAs compensated surface area created as a result of the sulfur passivation. Finally, the average value of the weak localization resistance drop appeared to be close to the period of the magnetoresistance oscillations.

References

[1] M.A. Kastner. Phys. Today, **46**, 24 (1993).
[2] C.T. Liang, M.Y. Simmons, S.G. Smith, G.H. Kim, D.A. Ritchie, M. Pepper. Phys. Rev. Lett., **81**, 3507 (1998).
[3] S. Nagaraja, P. Matagne, V.Y. Thean, J.P. Leburton, Y.H. Kim, R.M. Martin. Phys. Rev. B: Condens. Matter, **56** (24), 15 752 (1997).
[4] S. Tarucha, D.G. Austing, T. Honda. Phys. Rev. Lett., **77**, 3613 (1996).
[5] C.W.J. Beenakker. Phys. Rev. B, **44**, 1646 (1991).
[6] H. Grabert, M.H. Devoret. Single charge tunneling, coulomb blockade phenomena in nanostructures NATO. Adv. Sci. Inst. Ser. B, v. 294 (Plenum Press, N.Y., ISBN 0-306-44229-9, 1992).
[7] S. Tarucha, T. Honda, T. Saku. Sol. St. Commun., **94**, 413 (1995).
[8] N.N. Ledentsov. *Proc. of the 23rd Int. Conf. on Physics of Semiconductors* (22–27 July 1996, Berlin, Germany) ed. by M. Scheffler, R. Zimmermann (World Scientific, Singapore, 1996) v. 1, p. 19.
[9] T.J. Thornton, M. Pepper, H. Ahmed, D. Andrews, G.J. Davies. Phys. Rev. Lett., **56**, 1198 (1986).
[10] D.V. Lang, R.A. Logan. Phys. Rev. Lett. **39**, 635 (1977).
[11] S.L. Feng, J.C. Bourgoin. Sol. St. Fenom., **10**, 265 (1989).
[12] D.V. Averin, A.N. Korotkov, K.K. Likharev. Phys. Rev. B, **44**, 6199 (1991).
[13] D. Goldhaber-Gordon, H. Shtrikman, D. Mahalu, D. Abush-Magder, U. Meirav, M.A. Kastner. Nature, **391**, 156 (1998).
[14] N.T. Bagraev, L.E. Klyachkin, A.M. Malyarenko, W. Gehlhoff. Superlat. Microstr., **23**, 1333 (1998).
[15] N.T. Bagraev, A.D. Bouravlev, L.E. Klyachkin, A.M. Malyarenko, W. Gehlhoff, Yu.I. Romanov, S.A. Rykov. Semiconductors, **39**, 6, 685 (2005).
[16] D.K. Ferry, S.M. Goodnick, J. Bird. *Transport in Nanostructures* (Cambridge University Press, 2009).
[17] S.J. Shin, J.J. Lee, H.J. Kang, J.B. Choi, S.-R.E. Yang, Y. Takahashi, D.G.Hasko. Nano Lett., **11** (4), 1591 (2011).
[18] U. Meriav, E.B. Foxman. Semicond. Sci. Technol., **10**, 255 (1995).
[19] N.T. Bagraev, N.M. Kolchanova, V.A. Mashkov. JETP Lett., **45(5)**, 288 (1987).
[20] N.T. Bagraev. J. Phys. (France) I, **1**, 1511 (1991).
[21] N.T. Bagraev. Mater. Sci. Forum, **143**–**147**, 543 (1994).
[22] M. Martin, S. Makram-Ebeid. Physica, **116B**, 371 (1983).
[23] T. Figielski. Appl. Phys. A, **35**, 255 (1984).
[24] T. Figielski, T. Wosinski, A. Makosa. Acta Phys. Polonica A, **92** (4), 745 (1997).
[25] L. Esaki. Phys. Rev., **109** (2), 603 (1958).
[26] R.N. Thomas, H.M. Hobgood, G.W. Eldridge, D.L. Barrett, T.T. Braggins. Sol. St. Electron., **24** (5), 387 (1981).
[27] S. Makram-Ebeid. *Semi-insulating III−V materials* (Shiva Pub, Evian, 1982) p. 397.

[28] A. Kangarlu, H. Guarriello, F.L. Berney, P.W. Yu. Appl. Phys. Lett., **59**, 2290 (1991). K.R. Elliot. Appl. Phys. Lett., **42**, 274 (1983).

[29] P. Schultz, A. von Lilienfeld. Modelling Simul. Mater. Sci. Eng., **17**, 084 007 (2009).

[30] W.G. Schmidt, F. Bechstedt, J. Bernholc. Appl. Surf. Sci., **190**, 264 (2002).

[31] V.P. La Bella, M.R. Krause, Z. Ding, P.M.Thibado. Surf. Sci. Reports, **60**, 1 (2005).

[32] B.L. Altshuler, D. Khmel'nitzkii, A.I. Larkin, P.A. Lee. Phys. Rev. B, **22**, 5142 (1980).

[33] S. Datta. *Electronic Transport in Mesoscopic Systems* (Cambridge University Press, ISBN 0521599431, 1995).

[34] K.K. Choi, D.C. Tsui, K. Alavi. Phys. Rev. B, **36**, 7751(R) (1987).

[35] B.L. Al'tshuler, A.G. Aronov. JETP Lett., **33** (10), 499 (1981).

[36] S. Hikami, A.I. Larkin, Y. Nagaoka. Prog. Theor. Phys., **63** (2), 707 (1980).

[37] S.A. Studenikin, P.T. Coleridge, N. Ahmed, P.J. Poole, A. Sachrajda. Phys. Rev. B, **68**, 035 317 (2003).

[38] J.A. Simmons, D.C. Tsui, G. Weimann. Surf. Sci., **196**, 81 (1988).

[39] V.N. Bessolov, M.V. Lebedev. Semiconductors, **32** (11), 1141 (1998).

[40] E.Yu. Beliayev, B.I. Belevtsev, Yu.A. Kolesnichenko. Low Temperature Phys., **37**, 318 (2011).

[41] H.G. Johnson, S.P. Bennett, R. Barua, L.H. Lewis, D. Heiman. Phys. Rev. B, **82**, 085 202 (2010).

[42] M.M. Parish, P.B. Littlewood. Phys. Rev. B, **72**, 094 417 (2005).

[43] E.R. Viana, G.M. Ribeiro, A.G. Oliveira, M.L. Peres, R.M. Rubinger, C.P.L. Rubinger. Mater. Res., **15** (4), 530 (2012).

[44] B. Jabakhanji, A. Michon, C. Consejo, W. Desrat, M. Portail, A. Tiberj, M. Paillet, A. Zahab, F. Cheynis, F. Lafont, F. Schopfer, W. Poirier, F. Bertran, P. Le Fèvre, A. Taleb-Ibrahimi, D. Kazazis, W. Escoffier, B.C. Camargo, Y. Kopelevich, J. Camassel, B. Jouault. Phys. Rev. B, **89**, 085 422 (2014).

[45] D.W. Jung, J.P. Noh, A.Z.M.T. Islam, N. Otsuka. J. Phys. Soc. Jpn., **77**, 074 721-8 (2008).

Редактор К.В. Емцев